Hyperfine Interact (2009) 188:71–78
DOI 10.1007/s10751-008-9891-6

Spin-transition in nearly cubic site in $[Fe^{II}(L)_3][PF_6]_2$

Vibha Mishra · Rabindranath Mukherjee · Jorge Linares · Epiphane Codjovi · François Varret · Max Lawson-Daku

Published online: 28 October 2008

Abstract The spin-transition ($^1A_1 \leftrightarrow {}^5T_2$) behaviour of a new mononuclear iron(II) compound $[Fe^{II}(L)_3][PF_6]_2$[L = 2-[3-(2′-pyridyl)pyrazole-1-ylmethyl]pyridine] has been investigated by ^{57}Fe Mössbauer spectroscopy. Analysis of the Mössbauer spectra revealed low value of the quadrupole splitting of the high-spin state which reflects iron(II) to be in nearly cubic lattice site. Mössbauer spectra under light show the light-induced excited spin state trapping effect and the observed quadrupole splitting of the metastable high-spin state is found little sensitive to the high-spin fraction value. DFT calculations are in progress to document the almost cubic nature of the ligand-field acting on the iron atom.

Keywords Spin-transition · ^{57}Fe Mössbauer spectroscopy · Iron(II) complex · Ligand-field · Density functional theory

1 Introduction

Spin-transition [1] represents an important area of research due to its suggested importance in display/memory devices and optical switches. The present report stems from our continued research interest in exploring the spin-state properties

V. Mishra · R. Mukherjee (✉)
Department of Chemistry, Indian Institute of Technology Kanpur, Kanpur 208 016, India
e-mail: rnm@iitk.ac.in

V. Mishra · J. Linares · E. Codjovi · F. Varret
GEMAC, CNRS, Université de Versailles, 78035 Versailles cedex, France

F. Varret
e-mail: fvarret@physique.uvsq.fr

M. Lawson-Daku
Département de Chimie Physique, Université de Genève,
30 Quai Ernest Ansermet, 1211 Geneva 4, Switzerland
e-mail: max.lawson@unige.ch

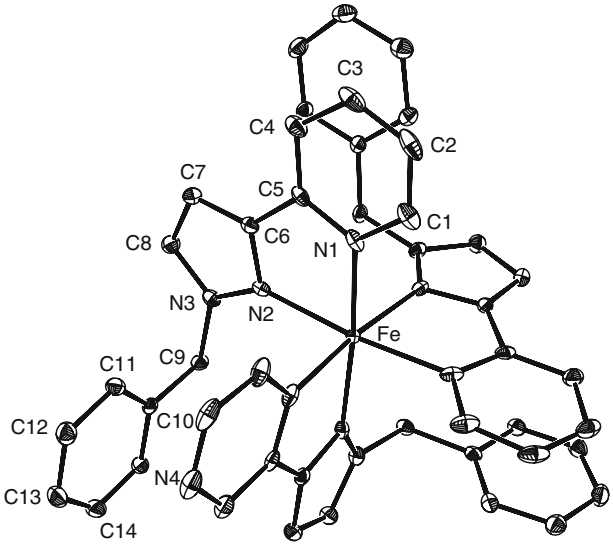

Fig. 1 Perspective view of crystallographically independent dication in the crystal of $[Fe^{II}(L)_3][PF_6]_2.2H_2O$ showing the atom numbering. Atoms are drawn at the 40% probability level. Hydrogen atoms are omitted for clarity. Unlabeled atoms are symmetry related to the labeled atoms

of mononuclear MN_6 octahedron iron(II) complexes with pyridine/pyrazole-based chelating ligands [2]. We show here on the example of $[Fe^{II}(L)_3][PF_6]_2{\cdot}2H_2O$ that three such ligands around the metal center may realize a highly symmetric environment, rarely observed so far ([3] reports the unique example of quasi-cubic octahedral iron(II) we found in Mössbauer literature) hence worth being investigated with some detail by Mössbauer spectroscopy. Such an environment is reported in Fig. 1.

2 Experimental

Single crystals of the complex $[Fe^{II}(L)_3][PF_6]_2{\cdot}2H_2O$ were obtained by recrystallization of $[Fe^{II}(L)_3][PF_6]_2{\cdot}2H_2O$ from MeOH-H_2O mixture (1:1) in 8–10 days. Details of the synthesis and structure (Fig. 1) will be stated elsewhere. The as-prepared crystals did not show spin-transition and subsequent drying was performed under vacuum with slight heating (40–50°C), leading to the powder samples investigated here. Mössbauer spectra were recorded on a constant-acceleration spectrometer, with a 50 mCi source of ^{57}Co in rhodium matrix. The polycrystalline absorber contained 20 mg of material/cm^2. The typical experimental line width, in the useful velocity range, was ~0.215 mm/s^{-1}. The spectra, once folded, were fitted without correction of the thickness effect. Irradiation was provided by a solid-state laser (25 mW, 532 nm) connected to a single piece optical fibre inserted along the sample holder rod. The merging beam was delivered to the sample by a mirror made of

Fig. 2 Selected ^{57}Fe Mössbauer spectra of $[Fe^{II}(L)_3][PF_6]_2$. The high-spin and low-spin contributions are highlighted with dark and light grey respectively. *Left side*: (**a–d**) 300, 120, 77, 30 respectively. *Right side*: 4.2 K, **e** before irradiation, **f** under light after 2 h irradiation, **g**, **h** subsequent decay in the dark, in the time intervals 0–7 h, 20–34 h respectively ▶

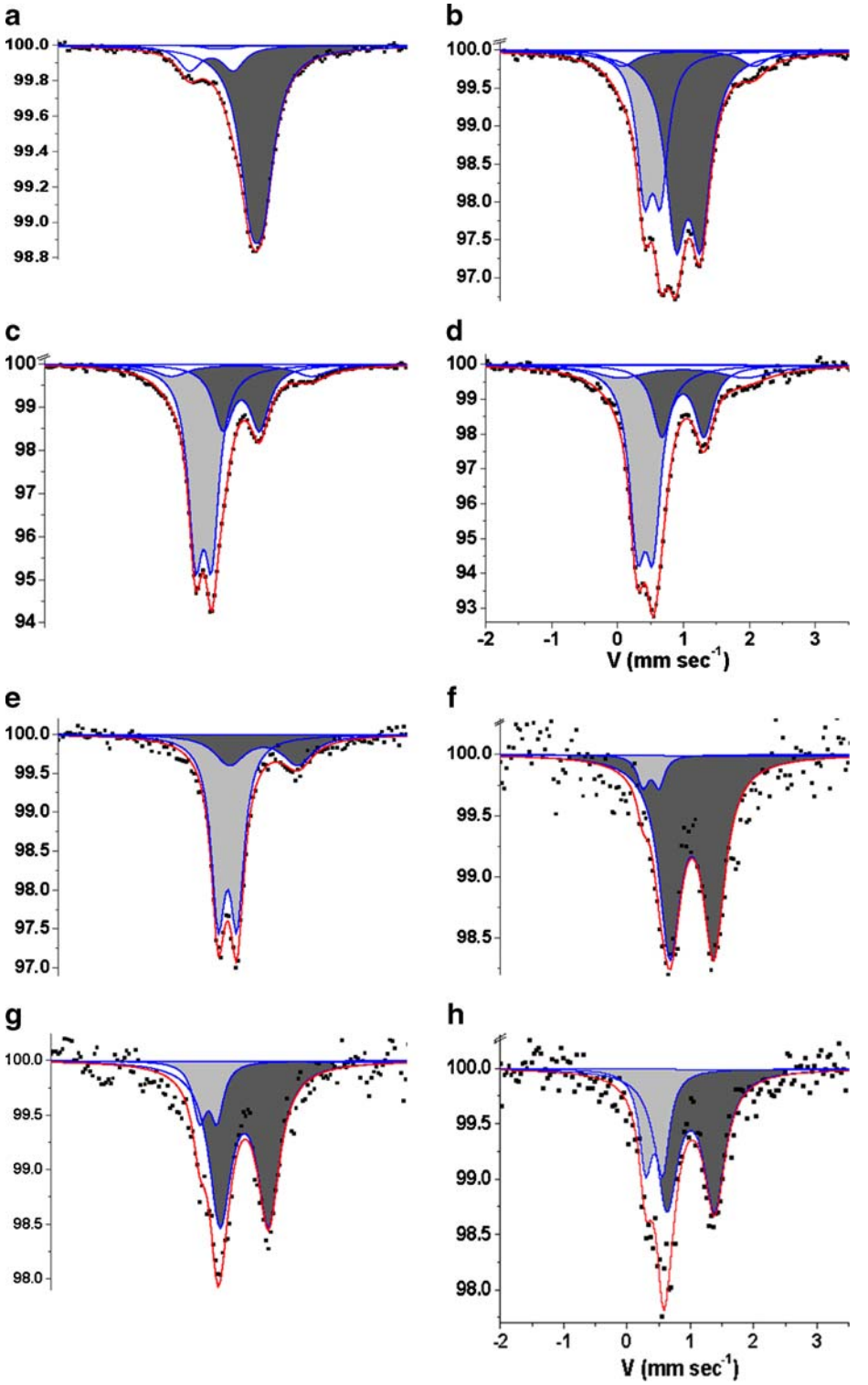
a
b
c
d
e
f
g
h
V (mm sec^{-1})
V (mm sec^{-1})

aluminized mylar sitting in the γ-ray pathway. Such a device did not significantly increase the liquid helium boiling rate of the cryostat.

3 Results and discussion

Selected Mössbauer spectra are shown in Fig. 2, and the complete set of fitted data is reported in Table 1. At 298 K (spectrum **a**) the main contribution is an unresolved doublet typical for high-spin Fe^{II} in quasi-cubic site (data in Table) with a weak doublet of high-spin Fe^{III} (Isomer shift δ = 0.33(1) mm/s, Quadrupole splitting ΔE_Q = 0.63(1) mm/s) assigned to a small amount of ferric hydroxide with the relative area of ∼15% which will drastically decrease at lower temperature due to the huge variation of the Lamb–Mössbauer factor of the spin-crossover contributions, as already noticed in [4] (the reader observe the changes in vertical scale). At lower temperatures (spectra b, c, d) spin equilibrium is observed with resolved quadrupole doublets. The high-spin contribution actually splits into a major contribution (dark grey) and a minor contribution (white) which might be assigned to a sizable admixture of polymorphic phase (Mishra, V. et al., manuscript under preparation) or local effects due to incomplete solvent removal. We controlled by recording Mössbauer spectra at a larger velocity scale that we were not dealing with the innermost lines of a sextet.

Magnetic measurements (Fig. 3) are consistent with the Mössbauer data and show a large freezing-in effect at low temperatures which will be treated in a further report at the light of kinetic experiments which are sketched as an inset to Fig. 3.

Photo-excitation was performed at 4.2 K using a thinner sample (∼5 mg on a 12 mm diameter disc). The spectra are reported in Fig. 2, right. Before irradiation, spectrum e shows little differences with respect to the thicker sample. The data are listed in Table 1, and the resulting discrepancies may be assigned to different cooling rates leading to different trapped HS fractions, and/or thickness effects which are known to be large in case of badly resolved lines (see [5] for example). After 2-h irradiation, spectrum f shows an almost complete transformation into the high-spin state. After switching off the light, the spectra were recorded during successive time intervals, and show a progressive decay towards the stable low-spin state (spectra g, h).

4 Discussion

The crucial features are the unusually low values of the quadrupole splitting of the (main) high-spin contribution, which reveal a very low value of the non-cubic components of the ligand-field at the iron site. The thermal variation is reported in Fig. 4 and could not be reproduced by the usual static ligand-field models [6, 7]. Alternatively, the strong variation in the range 50–150 K suggested a correlation with the high-spin fraction value, through the effect of local distortions associated with the spin conversion of the neighbouring molecular units. However, the photo-excitation experiment at low temperature showed that the QS value in the high-spin sites are little sensitive to the changes in the high-spin fraction. This surprising lack of sensitivity, compared to high-symmetry systems in Mössbauer literature (see [8, 9] for instance), might be presumably attributed to the chelating character of the ligands, able to hinder some of the possible distortions of the surroundings of the iron(II) atom.

Table 1 Least-square-fit parameters of $[Fe^{II}(L)_3][PF_6]_2$. IS, QS, Γ, respectively are the isomer shift referred to metallic iron at room temperature, quadrupole splitting, and Lorentzian line width

T(K)	IS(HS) (mm/s)	QS(HS) (mm/s)	Γ(HS) (mm/s)	% (±2)	IS(LS) (mm/s)	QS(LS) (mm/s)	Γ(LS) (mm/s)	% (±2)
4.2	1.164 (7)	0.71(1)	0.216(7)	32	0.548(2)	0.230(4)	0.360(5)	60
	1.164 (7)	*1.87(6)*	*0.50*	8				
30	1.125(5)	0.639(9)	0.33(2)	33	0.553(2)	0.242(3)	0.290(6)	59
	1.125(5)	*2.07(6)*	*0.50*	8				
77	1.123(3)	0.555(5)	0.36(6)	30	0.548(1)	0.247(2)	0.268(2)	61
	1.123(3)	2.15(3)	*0.50*	9				
90	1.120(4)	0.497(6)	0.34(1)	45	0.549(3)	0.244(3)	0.260(6)	46
	1.120(4)	*2.15(5)*	*0.50*	9				
100	1.116(3)	0.467(4)	0.368(6)	50	0.547(2)	0.255(2)	0.28(4)	44
	1.116(3)	*2.07(4)*	*0.50*	6				
110	1.112(3)	0.424(4)	0.370(6)	53	0.544(3)	0.258(3)	0.29(1)	40
	1.112(3)	*2.18(4)*	*0.50*	7				
120	1.106(2)	0.390(3)	0.390(4)	60	0.542(2)	0.256(3)	0.286(5)	33
	1.106(2)	*2.08(3)*	*0.486(4)*	7				
130	1.099(3)	0.347(3)	0.392(6)	64	0.543(4)	0.250(4)	0.31(1)	29
	1.099(3)	*2.08(4)*	*0.49(4)*	7				
140	1.097(3)	0.310(3)	0.398(6)	68	0.534(5)	0.262(5)	0.32(1)	25
	1.097(3)	*2.06(3)*	*0.50*	7				
150	1.091(3)	0.274(3)	0.388(6)	71	0.538(7)	0.278(7)	0.34(2)	22
	1.091(3)	*2.06(4)*	*0.50*	7				
200	1.050(3)	0.203(5)	0.40	81	0.452	0.29	0.34	7
	0.35(2)[a]	0.51(5)[a]	0.42(4)[a]	12				
250	1.025(3)	0.15(1)	0.40	86	0.452	0.29	0.34	2
	0.39(2)[a]	0.65(5)[a]	0.38[a]	12				
295 Fe^{III}(HS)	0.985(2)	0.18(1)	0.40	83	0.432	0.29	0.34	3
	0.33(1)[a]	0.64(3)[a]	0.37(2)[a]	15				

Table 1 (continued)

T(K)	IS(HS) (mm/s)	QS(HS) (mm/s)	Γ(HS) (mm/s)	% (±2)	IS(LS) (mm/s)	QS(LS) (mm/s)	Γ(LS) (mm/s)	% (±2)
4.2 K (irradiation)								
Before	1.157	0.79(3)	0.38	19	0.558(2)	0.265(4)	0.240(6)	72
	1.157	*2.1(1)*	*0.50*	9				
Under	1.145(9)	0.78(2)	0.460(2)	98	0.564	0.27	0.248	2
4.2 K after irradiation								
0–7 h	1.124(6)	0.75(1)	0.371(2)	74	0.564	0.27	0.248	26
7–20 h	1.147(7)	0.71(1)	0.360(2)	71	0.564	0.27	0.248	29
20–34 h	1.156(7)	0.73(1)	0.370(2)	66	0.564	0.27	0.248	34

Minor contributions are *italicized*. Standard deviations of statistical origin are given in *brackets*. In case of overlapped lines, we constrained the most sensitive parameters (*underlines values*)

[a] ferric hydroxide component

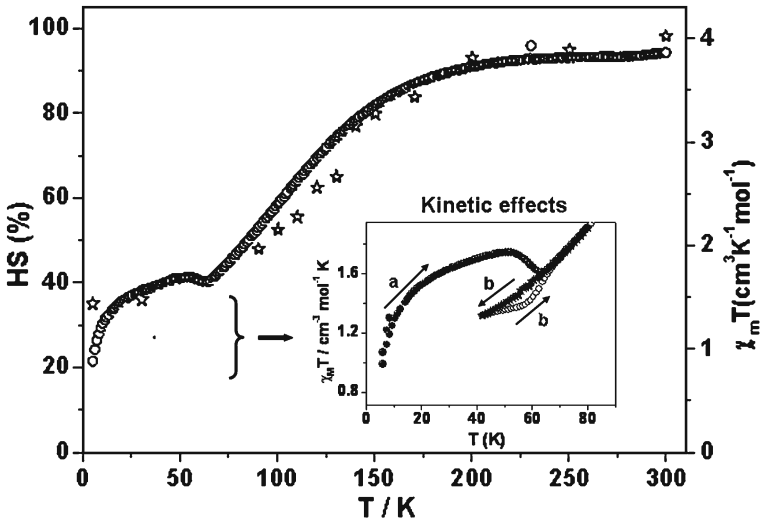

Fig. 3 The spin equilibrium of $[Fe^{II}(L)_3][PF_6]_2$ from SQUID magnetization data under 1 kOe in the warming mode (*open circle*) and from Mössbauer investigation (*star*). The magnetic curve exhibits zero-field-splitting effect at low temperature and evidences freezing-in below ~60 K, as confirmed by kinetic experiments plotted in *inset*: warming from thermally quenched state (*a*), slow cooling and warming (*b*)

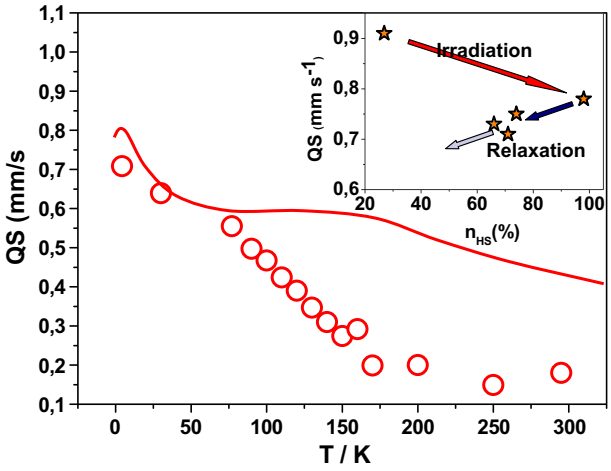

Fig. 4 The quadrupole splitting data of the high-spin main contribution of $[Fe^{II}(L)_3][PF_6]_2$, as a function of temperature (*open circle*) and as a function of high-spin fraction (*star*; as *inset*). Full line is reproduced from static crystal field model, adapted from [6]

DFT studies were undertaken in order to document the quasi-cubic character of the ligand field, using the ADF program package [10, 11]. First, the geometry of the complex was optimized in the HS and the LS states; then, for the determination of the EFG at the iron center, scalar relativistic calculations were performed in the zero-order regular approximation on the optimized HS and LS structures. Details will be provided in a specific report. Contrarily to the experimental observations reported above, the isolated complex is predicted to be HS at all temperatures, with a calculated HS-LS electronic energy difference of −2,359 cm^{-1}. Furthermore the

computed quadrupole splitting value of ~3.5 mm s^{-1} is far too large, compared to the experimental value, and it is predicted to be almost temperature-independent. The present discrepancy can be mainly ascribed to the fact that spin-orbit coupling and crystal packing effect are neglected in our computations performed on the complex in the gas phase. Indeed, spin-orbit coupling is probably responsible for the admixing of the other components of the ligand-field $^5T_2$ state into the HS ground state; these ones being given at 3,302 and 4,083 cm^{-1} above the HS ground state by electronic excitation calculations carried out within time-dependent DFT (TDDFT). Crystal packing effect may bring the HS component closer in energy, thus making the admixing due to the spin-orbit coupling more effective. As a matter of fact, the hydrated compound remains HS at all temperatures, with a quadrupole splitting value of ~1.4 mm s^{-1} at room temperature (~2.05 mm s^{-1} at 77 K).

Acknowledgements We acknowledge CEFIPRA (contract IFC 3408-3) for the post-doctoral grant of Vibha Mishra.

References

1. Gütlich, P., Goodwin, H. (Eds.): Spin crossover in transition metal compounds. Topics in current chemistry, vols. 233–235. Springer, Berlin (2004)
2. Singh, S., Mishra, V., Mukherjee, J., Seethalekshmi, N., Mukherjee, R.: Synthesis and properties of $[M^{II}(L^6)_2][ClO_4]_2$ (M = Fe, Co and Ni): structures of Co and Ni complexes and spin-state transition by Fe complex (L^6 = 2-[3-(2′-pyridyl)pyrazol-1-ylmethyl]pyridine). Dalton Trans. **17**, 3392–3397 (2003)
3. Frankel, R.B., Chappert, J., Regnard, J.R., Misetich, A., Abeledo, C.R.: Electronic properties of Fe^{2+} in cubic $KMgF_3$ from Mössbauer spectroscopy. Phys. Rev., B. **5**, 2469–2474 (1972)
4. Gressier, J.C., Levesque, G., Patin, H., Varret, F.: Polymer-supported transition-metal complexes. 2. Synthesis and Mössbauer investigation of copolymers containing polynuclear iron carbonyl complexes. Macromolecules **16**, 1577–1581 (1983)
5. Oosterhuis, W.T., Lang, G.: Mössbauer effect in K_3FeCN_6. Phys. Rev. **178**, 439 (1969)
6. Ingalls, R.: Electric-field gradient tensor in ferrous compounds. Phys. Rev. **133**, A787–A795 (1964)
7. Varret, F.: Crystal-field effects on high-spin ferrous ion. J Physique France **37**(C6), 437–456 (1976)
8. Gerard, A., Imbert, P., Prange, H., Varret, F., Winterberger, M.: Fe^{2+} Impurities, isolated and in pairs, in ZnS and CdS studied by the Mössbauer effect. J. Phys. Chem. Solids **32**, 2091–2100 (1971)
9. Bonville, P., Garcin, C., Gerard, A., Imbert, P., Jehanno, G.: Mössbauer absorption and emission study of dilute Fe^{2+} impurities in cubic ZnS. Observation of metastable electronic levels. I. Relaxation measurements. Phys. Rev., B. **23**, 4293–4309 (1981)
10. te Velde, G., Bickelhaupt, F.M., Baerends, E., Fonseca Guerra, C., van Gisgergen, S.J.A., Snijders, J.G., Ziegler, T.J.: Chemistry with ADF. Comput. Chem. **22**, 931–967 (2001)
11. Amsterdam Density Functional. Release ADF2004.01, Theoretical chemistry, Vrije Universiteit, the Netherlands. http://www.scm.com